SAND2016-1917J

Effects of Coarse-Graining Level on Dynamic Properties of Polymeric Materials

K. Michael Salerno,[1,*] Anupriya Agrawal,[2,†] Dvora Perahia,[2] and Gary S. Grest[1]

[1] *Sandia National Laboratories, Albuquerque, NM, 87185*

[2] *Department of Chemistry, Clemson University, Clemson, SC 29634*

Coarse-grained models access large length and time scales by combining groups of atoms into beads or superatoms while retaining some atomistic details. Using linear polyethylene as a model system, we show how the coarse-graining scale affects the measured properties of the system. Iterative Boltzmann inversion is used to derive coarse-grained potentials with 2, 3, 4 or 6 methylene groups per coarse-grained bead from a fully atomistic polyethylene melt simulation. The dynamics of these four models are 6-10 times faster than in atomistic simulations due to the smoother free energy landscape. While the coefficient of thermal expansion and plateau modulus depend only weakly on the degree of coarse graining, the crystallization temperature depends strongly on the degree of coarse graining. Using these coarse-grained models we are able to simulate melts of $C_{1920}H_{3842}$ chains for times longer than 200 μs to study the long-time behavior of well-entangled polymer chains.

Polymer properties depend on a wide range of coupled length and time scales, with unique viscoelastic characteristics stemming from interactions at the atomistic level. The need to probe polymers across time and length scales makes computational modeling inherently challenging. With increasing molecular weight, polymer melts become highly entangled and the long-time diffusive regime becomes computationally inaccessible using atomistic simulations. In these systems the diffusive time scale increases with polymerization number N faster than N^3, becoming greater than 10^{10} times larger than the shortest time scales even for modest molecular weight polymers. The challenge is to develop a model that captures important atomistic details and can simulate long polymer chains over very long time scales.

One path to overcoming this challenge is to coarse grain the polymer, thereby reducing the number of degrees of freedom and increasing the fundamental time scale. The process of coarse graining amounts to combining groups of atoms into pseudoatom beads and determining appropriate interaction potentials [1]. Simple models such as the bead-spring model [2], capture characteristics described by scaling theories, but disregard atomistic details and cannot quantitatively describe properties such as structure, local dynamics or densities. Immense efforts have been made to coarse grain polymers and bridge the gap of time and length scales, while retaining atomistic characteristics. Using this procedure, much larger time and length scales can be accessed while maintaining a connection to the atomistic details of the polymer [3]. One critical issue underlying the coarse graining process is the degree to which a polymer can be coarse grained and still appropriately capture the properties and dynamics of the polymer. The current study uses simulations to probe the effects of the degree of coarse graining of polymers on their properties.

With the immense efforts to coarse grain polymers, several models have emerged whose differences lie in the number of atoms captured by each bead and the procedure for determining the interaction potentials. One of the most common coarse-grained (CG) models for polymers is united atom (UA) model, which combines each CH_n group into a pseudoatom. The UA interaction parameters are determined phenomenologically to reproduce physical properties such as densities and critical temperatures [4–7]. Another model commonly used is the MARTINI model, which utilizes the same approach, matching bulk densities and compressiblities of short alkane chains at a larger scale of four CH_2 groups per CG bead.[8] More advanced methods such as force matching, iterative Boltzmann inversion, and optimized relative entropy [9–11] have recently been developed to incorporate atomistic detail into the CG model. With these methods there is still an open question as to the optimum number of atoms to represent by a single bead and its effect on the measured properties of the system.

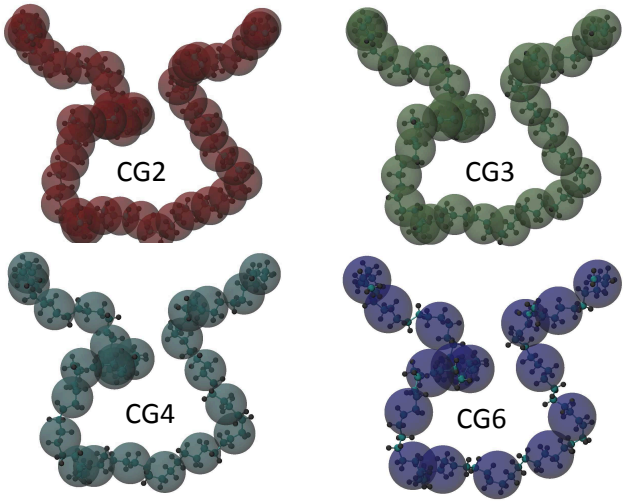

FIG. 1. A single $C_{96}H_{194}$ PE chain represented with increasing degree of coarse graining λ = 2, 3, 4, and 6 methylene groups per CG bead.

Here, we develop CG models with varying degree of coarse graining using iterative Boltzmann inversion. We study how well these CG models describe both the

static and dynamic properties of a polymer melt, using polyethylene (PE) as a model system. The backbone of PE consists of -CH_2- methylene groups that provide a natural unit or scale for coarse graining. Though the chemical structure of PE is simple, it is a thermoplastic material used in a large number of applications, with its mechanical properties determined by the degree of branching.

Polyethylene chains have been previously studied using CG models with beads of $\lambda = 3-48$ methylene groups per bead [12–17]. These studies were able to capture the radius of gyration as a function of molecular weight and the pair correlation function between CG beads. As most of these studies used a large degree of coarse graining ($\lambda \sim 20$) to study dynamical properties, an extra constraint was needed to prevent chains cutting through each other [18]. With this extra constraint, the mean squared displacement (MSD), stress autocorrelation function and shear viscosity of linear and branched PE [18–20] have been studied for long, entangled chains. However, these studies did not account for or study the effects of the coarse-graining degree λ on dynamic properties.

Here for the first time, we elucidate the effects of coarse-graining degree on the ability to capture both the structure and dynamics of PE. We are able to capture the dynamics of polymer chains of length up to $C_{1920}H_{3842}$ for time scales of order 200 μs using models that accurately represent atomistic detail. By accessing these large length and time scales we are able to measure quantities like the plateau modulus which depend on a hierarchy of length and time scales.

Coarse-grained beads shown in Fig. 1 represent λ methylene groups. Here we study $\lambda = 2$, 3, 4 and 6 and refer to these models as CGλ. We find that for a surprising small λ, as small as CG6, an additional soft segmental repulsive interaction is required between each pair of bonded beads to enforce non-crossing of the chains. We include the CG6 model in our study to compare with smaller bead models, but do not model larger CG beads.

The CG PE potentials were derived from a single fully-atomistic simulation of a melt of $C_{96}H_{194}$ PE chains at 500K. The simulation details are given in the Supplement. The study was then generalized to melts of C_nH_{2n+2} with n=96, 480 for the fully atomistic model, and n=96, 480, 960 and 1920 using the CG models. Atomistic simulations used a modified version of the Optimized Potentials for Liquid Simulations (OPLS) potential with modified dihedral potential coefficients that better reproduce the properties of long alkane chains [21]. With this modified potential the mean squared radius of gyration $\langle R_g^2 \rangle$ and end to end distance $\langle R^2 \rangle$ match experimental values [22, 23] better than with the original OPLS parameters [24]. For the CGλ models, the end to end distance $\langle R^2 \rangle$ for n=96 chains is within 20% of the atomistic value, while $\langle R^2 \rangle$ for the MARTINI model is about 50% too high. Measurements of static properties for different chain lengths are reported in the Supplement.

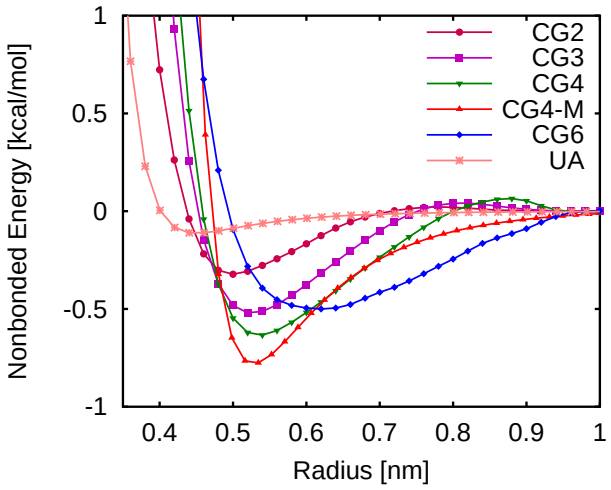

FIG. 2. Pair potential between CG beads. The UA and CG4-M potentials are included for comparison.

The CG angle and bond potentials were determined by Boltzmann inversion of the atomistic bond and angle distributions shown in Fig. S1. Torsion terms were omitted in all CG models, which may account for the shorter end to end distances listed in Table SI for the CG2 model. The bond and angle potentials were determined by iterative Boltzmann inversion [3]. The intermolecular radial distribution function g(r) shown in Fig. S2 determined from the atomistic simulation was used as the target for iteration of the pair potential between CG beads. The resulting pair potentials are shown in Fig. 2. Also shown are the 6-12 Lennard Jones pair potentials for the united atom (UA) model of Yoon et al. [4], as well as the MARTINI (CG4-M) model.[8] In our simulations the MARTINI parameter ϵ was reduced from $\epsilon = 0.8365$ kcal/mol to $\epsilon = 0.803$ kcal/mol so that the system has the same density $\rho = 0.72$ g/cm^3 as our atomistic simulations for $C_{96}H_{194}$ chains. For each CG model a pressure correction is applied so that each model has density $\rho = 0.72$ g/cm^3 for n=96. The similarity in length and energy scales between the CG4 and CG4-M models is visible in Fig. 2. For all the CGλ models the end beads and inner beads are treated with the same interaction potential, however the mass of the end beads is higher by that of a hydrogen atom.

Surprisingly, the CG6 model has a large equilibrium bond distance relative to the bead diameter. Therefore a modified soft segmental repulsive potential [25] was added between CG beads to inhibit chain crossing. We used a segmental bead diameter of 0.5 nm. This scheme increases the pressure in our samples by about 80 atm at fixed density compared to simulations with no crossing constraint. Due to the reduction in number of degrees of

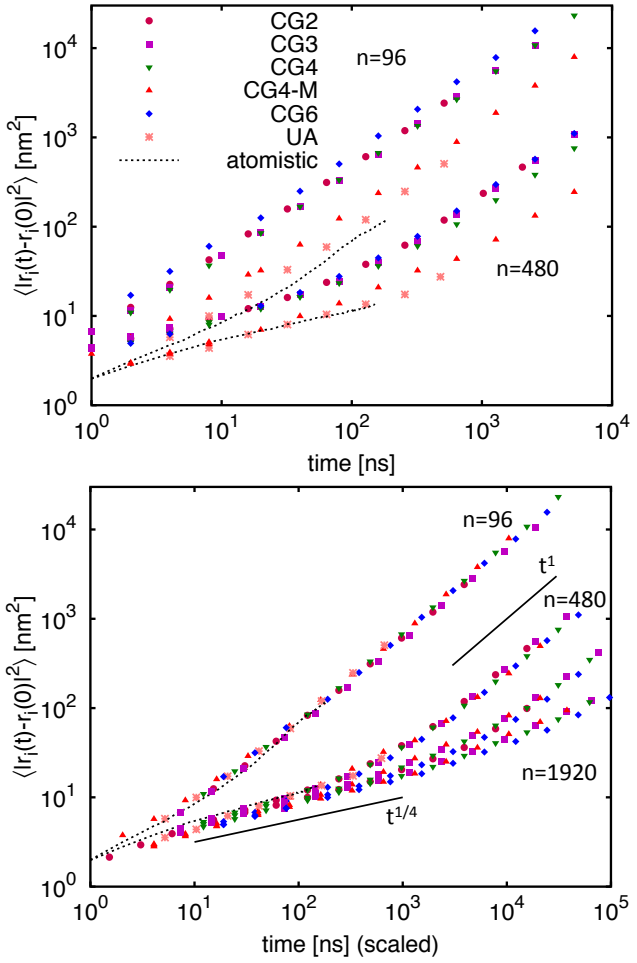

FIG. 3. (a) The MSD of the inner 24 methylene groups of each polymer chain. (b) Same data as in (a), scaled by α. The solid lines represent the scaling predictions t^1 for the long time diffusive time and $t^{1/4}$ for the reptation regime

freedom, CG models allow a significantly larger time step than atomistic models. Here we have used a time step δt = 20 fs for the CG6, CG4 and CG4-M models, 10 fs for the CG3 model and 2 fs for the CG2 model, compared to 1 fs for the fully atomistic model.

Coarse graining reduces the number of degrees of freedom in a system, creating a smoother free-energy landscape compared with fully atomistic simulations. It has been shown that this leads to CG dynamics that can be significantly faster than their atomistic counterparts [26–32]. To determine the dynamic scaling factor of the CG models we compared the mean squared displacement of the inner 24 methylene groups (4, 6, 8 or 12 beads) for CG models and the inner 24 carbon atoms for atomistic simulations for n=96 and 480 as shown in Fig. 3 (a). As expected, the mobility of the chains in the CG models is larger than for the atomistic simulation. By scaling the time for each of the CG models we can create a single collapsed curve each chain length for both the atomistic and CG monomer MSD data as shown in Fig.3 (b). The time shift α required to collapse the atomistic and CG data also collapses the $n = 960$ and 1920 data. Notably, a single scaling factor α has been applied for each CG model, independent of chain length. As seen in Fig. 3b the MSD has reached the diffusive regime where MSD $\sim t^1$ even for the longest chain length $n = 1920$. Over the intermediate time scales, the chains show the expected $t^{1/4}$ scaling predicted by reptation theory [33]. These results demonstrate that one can capture long time and length scales with CG models that account for the atomistic characteristics of the system.

The MSD of the center of mass was then measured to test the scaling factor α. Figure 4 shows the MSD of the polymer chain center of mass for chain lengths n=96, 480, 960, and 1920. These data have been scaled by the same α as for the MSD of the center methylene groups. The scale factor α as a function of CG model is shown inset in Fig. 4 along with α for the MARTINI [8] and UA [4] models. Our CG potentials have a significantly larger time scaling factor than either the MARTINI or UA models, similar to the time-scaling factor determined previously by Depa and Maranas for PE for a single value of λ.[27] Values of the time-scaling factor are also of the same order as those previously calculated for polystyrene modeled at a similar coarse-graining level.[31] The UA model has long been considered approximate to the fully-atomistic simulation and indeed is only ≈40% faster than the fully-atomistic simulation. Interestingly, the time scaling factor is not monotonic in CG level, with the CG2 and CG6 models exhibiting the largest speedup. This feature can be related to the potential well depths shown in Fig. 2, with the shallowest potentials associated with the largest value of α, as described previously by Depa and Maranas.[27]

The polymer entanglement mass M_e governs a number of properties of the polymer chain and provides information about mobility within the polymer mesh. Experimentally, $M_e = \frac{\rho RT}{G_N^0}$ is determined from the plateau modulus G_0^N of the stress relaxation function $G(t)$ [22]. Experimental values for polyethylene range from 1.6-2.5 MPa, corresponding to an entanglement mass of 1300-2000 g/mol [22, 23, 34, 35].

The relaxation modulus in each of our CG models was measured for the four different chain lengths via equilibrium stress correlations using the Green-Kubo relation $G(t) = (V/k_BT)\langle\sigma_{\alpha\beta}(t)\sigma_{\alpha\beta}(0)\rangle$ where $\sigma_{\alpha\beta}$ are the off-diagonal components xy, xz, and yz of stress. Figure 5 shows the stress relaxation modulus for each of the CG models for n=96 and 480 and for $\lambda \geq 3$ for n = 1920. The times for each CG model have been scaled by the corresponding α time scaling factor. Though it shows similar behavior, the UA model is omitted because the zero-pressure density is higher than the other models, making comparison difficult. The curves collapse for the short-

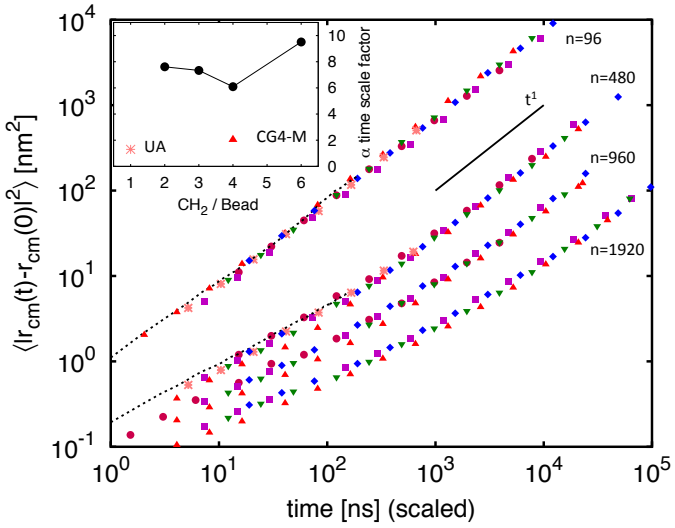

FIG. 4. Mean squared displacement of center of mass scaled with the same α scale factor as the MSD of the inner methylene groups in Fig. 3 (b). The solid line has slope t^1. Inset: The alpha scale factor for the different coarse-grained models and the UA and Martini models.

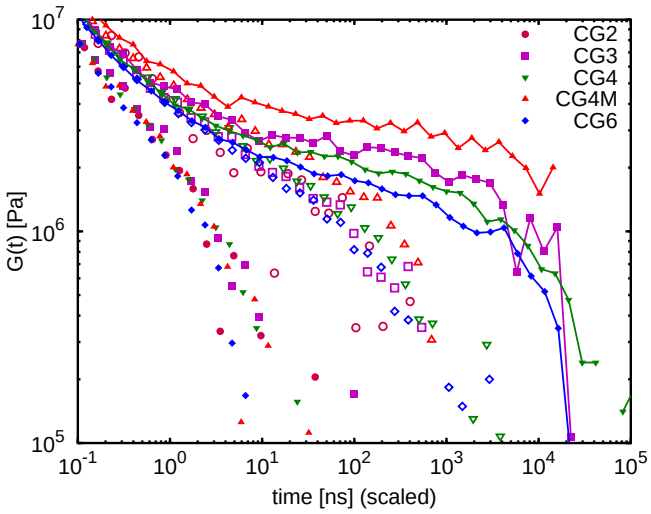

FIG. 5. Modulus $G(t)$ for each of the CG polymer models. Filled and open symbols represent the n=96 and n=480 chain length, respectively. Solid lines represent the n=1920 chain length, while n=960 chains are omitted for clarity.

time $t^{-1/2}$ regime, with longer, more entangled chains forming progressively more distinct plateau regions. The plateau modulus is measured as the value of the relaxation modulus in the plateau region. Using the longest chain length, n = 1920, the plateau modulus measured from the CGλ models is $G_N^0 = 1.6 \pm 0.2$ MPa for the CG6 model, $G_N^0 = 2.5 \pm 0.75$ MPa for the CG3 and $G_N^0 = 2.2 \pm 0.5$ MPa for the CG4 model, all within the experimental range. For the CG4-M model the measured plateau modulus is significantly higher $G_N^0 = 3.0 \pm 0.3$

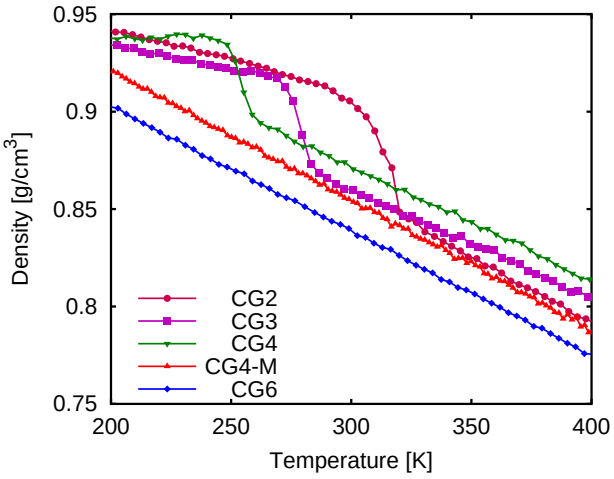

FIG. 6. Density versus temperature for the n=96 samples cooled at 1.4K/ns.

MPa and does not agree with experimental values. Uncertainties are measured by dividing the datasets into two and measuring the variation in the plateau value for each model. Similar values for the plateau modulus were calculated by Padding and Briels [18] for $n \leq 1000$ with $\lambda = 20$ model with a non-crossing constraint. We note that for each of the CG models except the MARTINI model, the plateau value is within the range of the experimental values. Measurement of the plateau modulus is only possible because our CG models allow us to simulate the longest chain lengths to hundreds of microseconds.

Measuring the thermal expansion coefficient is another way to assess the validity of the CG models. The linear thermal expansion coefficients for the n=96 samples in the temperature range from 495K to 480K are 5.0, 3.4, 3.5, 3.3, 3.4 $\times 10^{-4} T^{-1}$ respectively for the CG2, CG3, CG4, CG4-M, and CG6 models, compared with $3.1 \times 10^{-4} T^{-1}$ for the atomistic model. Hence, all the CG models with $\lambda \geq 3$ are in good agreement with the thermal expansion from the atomistic simulation.

Although it is possible to derive CG potentials using multiple state-points [36], our CG models are developed in the traditional way at single state point. Hence there is uncertainty about the validity of these models away from the chosen point [37]. Shown in Fig. 6 are temperature-density data for the CG models from 400K to 200K. For the CG2, CG3 and CG4 models the curves show a pronounced density increase between 250K and 330K, corresponding to an ordering of the sample to a crystalline phase. The CG6 model does not capture crystallinity and we expect that coarser models will not, either. Previous studies of simple bead-spring polymer models indicate that commensurate length scales between the bond length and bead size can lead to crystallization [38]. This surprising feature indicates that even though our potentials were derived at 500K they may have validity away

from this temperature. The melting temperature for n=96 chain is about 400K, so the crystallization occurs at a lower temperature than it should, yet it is remarkable that we observe a semi-crystalline phase at all. We intend to investigate the transferability of these CG PE potentials by reparameterizing the CG potentials at different temperatures for comparison in future studies.

The main goal of coarse-graining is to reach larger length and time scales by reducing the computational requirements of a given problem. The CG potentials developed here successfully capture the properties of PE and appropriate dynamics within entangled melts, allowing us to better model entanglements in real polymer systems. As described above, the CG6 model requires a non-crossing constraint which effectively doubles the number of sites, making it equivalent to a CG3 model, with respect to computational efficiency. This makes the CG4 model the most computationally efficient, reducing the number of degrees of freedom by more than a factor of 10. Both the CG6 and CG4 model allow a time step of 20 fs which, combined with the CG4 α time scaling factor the total computational reduction is greater than three orders of magnitude, enabling simulations of long, entangled chains for time scales approaching milliseconds. In fact, simulations of our longest chain lengths require only about 200,000 cpu core-hours on current processors.

The CG models of PE developed and tested capture static polymer properties. Further, monomer and polymer dynamics match atomistic simulations when a time scaling factor is applied. This time scaling factor can be deduced from either monomer or polymer diffusion data and ranges from 6-10, depending on model. Values of static properties like the end to end distance and entanglement length match between the CG models and atomistic simulations. The CG models developed here provide significant computational speedup over atomistic or united atom models while preserving dynamic and static properties, allowing large length and time scales to be reached.

ACKNOWLEDGEMENTS

AA and DP gratefully acknowledge financial support from Grant No. DE-SC007908 and a generous allotment of time on the Clemson University Palmetto cluster. This research used resources at the National Energy Research Scientific Computing Center (NERSC), which is supported by the Office of Science of the United States Department of Energy under Contract No. DE-AC02-05CH11231. This work was supported by the Sandia Laboratory Directed Research and Development Program. Research was carried out in part, at the Center for Integrated Nanotechnologies, a U.S. Department of Energy, Office of Basic Energy Sciences user facility. Sandia National Laboratories is a multi-program laboratory managed and operated by Sandia Corporation, a wholly owned subsidiary of Lockheed Martin Corporation, for the U.S. Department of Energy's National Nuclear Security Administration under contract DE-AC04-94AL85000. We acknowledge computational resources at the National Energy Research Scientific Computing Center, which is supported by the Office of Science of the United States Department of Energy, under Contract No. DE-AC02- 05CH11231.

* kmsaler@sandia.gov
† Current address: Department of Mechanical Engineering and Materials Science, Washington University, St. Louis, MO 63130

[1] S. O. Nielsen, C. F. Lopez, G. Srinivas, and M. L. Klein, Journal of Physics: Condensed Matter **16**, R481 (2004).
[2] K. Kremer and G. S. Grest, The Journal of Chemical Physics **92**, 5057 (1990).
[3] F. Müller-Plathe, ChemPhysChem **3**, 754 (2002).
[4] W. Paul, D. Y. Yoon, and G. D. Smith, The Journal of Chemical Physics **103**, 1702 (1995).
[5] S. K. Nath, F. A. Escobedo, and J. J. de Pablo, The Journal of Chemical Physics **108**, 9905 (1998).
[6] M. G. Martin and J. I. Siepmann, The Journal of Physical Chemistry B **102**, 2569 (1998).
[7] M. Mondello and G. S. Grest, The Journal of Chemical Physics **103**, 7156 (1995).
[8] S. J. Marrink, H. J. Risselada, S. Yefimov, D. P. Tieleman, and A. H. de Vries, The Journal of Physical Chemistry B **111**, 7812 (2007).
[9] S. Izvekov and G. A. Voth, The Journal of Physical Chemistry B **109**, 2469 (2005).
[10] M. S. Shell, The Journal of Chemical Physics **129**, 144108 (2008).
[11] V. Rühle and C. Junghans, Macromolecular Theory and Simulations **20**, 472 (2011).
[12] H. Fukunaga, J.-i. Takimoto, and M. Doi, The Journal of Chemical Physics **116**, 8183 (2002).
[13] J. T. Padding and W. J. Briels, The Journal of Chemical Physics **115**, 2846 (2001).
[14] H. S. Ashbaugh, H. A. Patel, S. K. Kumar, and S. Garde, The Journal of Chemical Physics **122**, 104908 (2005).
[15] X. Guerrault, B. Rousseau, and J. Farago, The Journal of Chemical Physics **121**, 6538 (2004).
[16] L.-J. Chen, H.-J. Qian, Z.-Y. Lu, Z.-S. Li, and C.-C. Sun, The Journal of Physical Chemistry B **110**, 24093 (2006).
[17] D. Curcó and C. Alemán, Chemical Physics Letters **436**, 189 (2007).
[18] J. T. Padding and W. J. Briels, The Journal of Chemical Physics **117**, 925 (2002).
[19] J. T. Padding and W. J. Briels, The Journal of Chemical Physics **118**, 10276 (2003).
[20] L. Liu, J. T. Padding, W. K. den Otter, and W. J. Briels, The Journal of Chemical Physics **138**, 244912 (2013).
[21] S. W. I. Siu, K. Pluhackova, and R. A. Böckmann, Journal of Chemical Theory and Computation **8**, 1459 (2012).
[22] L. J. Fetters, D. J. Lohse, S. T. Milner, and W. W. Graessley, Macromolecules **32**, 6847 (1999).

[23] L. J. Fetters, D. J. Lohse, and W. W. Graessley, Journal of Polymer Science Part B: Polymer Physics **37**, 1023 (1999).
[24] W. L. Jorgensen, D. S. Maxwell, and J. Tirado-Rives, J. Am. Chem. Soc. **118**, 11225 (1996).
[25] T. W. Sirk, Y. R. Slizoberg, J. K. Brennan, M. Lisal, and J. W. Andzelm, The Journal of Chemical Physics **136**, 134903 (2012).
[26] P. Depa, C. Chen, and J. K. Maranas, The Journal of Chemical Physics **134**, 014903 (2011).
[27] P. K. Depa and J. K. Maranas, The Journal of Chemical Physics **123**, 094901 (2005).
[28] I. Y. Lyubimov and M. G. Guenza, The Journal of Chemical Physics **138**, 12A546 (2013).
[29] I. Y. Lyubimov, J. McCarty, A. Clark, and M. G. Guenza, The Journal of Chemical Physics **132**, 224903 (2010).
[30] V. Harmandaris, Korea-Australia Rheology Journal **26**, 15 (2014).
[31] V. A. Harmandaris and K. Kremer, Soft Matter **5**, 3920 (2009).
[32] D. Fritz, K. Koschke, V. A. Harmandaris, N. F. A. van der Vegt, and K. Kremer, Phys. Chem. Chem. Phys. **13**, 10412 (2011).
[33] P. G. de Gennes, The Journal of Chemical Physics **72**, 4756 (1980).
[34] J. F. Vega, S. Rastogi, G. W. M. Peters, and H. E. H. Meijer, Journal of Rheology **48**, 663 (2004).
[35] V. R. Raju, G. G. Smith, G. Marin, J. R. Knox, and W. W. Graessley, Journal of Polymer Science: Polymer Physics Edition **17**, 1183 (1979).
[36] T. C. Moore, C. R. Iacovella, and C. McCabe, The Journal of Chemical Physics **140**, 224104 (2014).
[37] P. Carbone, H. A. K. Varzaneh, X. Chen, and F. Mller-Plathe, The Journal of Chemical Physics **128**, 064904 (2008).
[38] R. S. Hoy and N. C. Karayiannis, Phys. Rev. E **88**, 012601 (2013).